

Supporting information for the paper:

Au₂₂Ir₃(PET)₁₈ : An Unusual Alloy Cluster through Intercluster Reaction

Shridevi Bhat,^{†a} Ananya Bakshi,^{†a} Sathish Kumar Mudedla,^b Gana Natarajan,^a V. Subramanian,^b and Thalappil Pradeep^{*a}

*^aDST Unit of Nanoscience (DST UNS) and Thematic Unit of Excellence,
Department of Chemistry, Indian Institute of Technology Madras,
Chennai 600036, India.*

^bChemical Laboratory, CSIR-Central Leather Research Institute, Adyar, Chennai- 600020

† Equal contribution

Table of Contents

Name	Description	Page No.
SI 1	Materials and methods	S2
SI 2	Instrumentation	S4
Figure S1	Characterization of Au ₂₅ (PET) ₁₈	S6
Figure S2	Characterization of Ir ₉ (PET) ₆	S7
Figure S3	Effect of reactant concentration on the reaction	S8
Figure S4	Structure of Au ₂₅ (SMe) ₁₈	S9
Figure S5	DFT optimized structures of Au ₂₄ Ir(SMe) ₁₈ and Au ₂₃ Ir ₂ (SMe) ₁₈	S10
Figure S6	DFT optimized structures of lower energy isomers of Au ₂₂ Ir ₃ (SMe) ₁₈	S11
Figure S7	DFT optimized structures of higher energy isomers of Au ₂₂ Ir ₃ (SMe) ₁₈	S12
Table S1	Isomers of Au ₂₄ Ir ₁ (SMe) ₁₈ and their energies	S13
Table S2	Isomers of Au ₂₃ Ir ₂ (SMe) ₁₈ and their energies	S13
Table S3	Lower energy isomers of Au ₂₂ Ir ₃ (SMe) ₁₈ and their energies	S13
Table S4	Higher energy isomers of Au ₂₂ Ir ₃ (SMe) ₁₈ and their energies	S14
Figure S8	Result of TDDFT calculations	S15

Supporting information 1

Materials and Methods

Materials: Chloroauric acid trihydrate ($\text{HAuCl}_4 \cdot 3\text{H}_2\text{O}$), iridium(III) chloride hydrate ($\text{IrCl}_3 \cdot x\text{H}_2\text{O}$), 2-phenylethanethiol (PET), tetraoctylammonium bromide (TOAB), sodium borohydride (NaBH_4), Cesium acetate (CsOAc) and 2,5-dihydroxybenzoic acid (DHB) were purchased from Sigma Aldrich. Toluene, tetrahydrofuran (THF), dichloromethane (DCM) and methanol were purchased from Rankem and were of analytical grade.

Synthesis of clusters

Synthesis of $\text{Au}_{25}(\text{PET})_{18}$: $\text{Au}_{25}(\text{PET})_{18}$ was synthesized by the modified Brust – Schiffrin single phase synthesis protocol.¹ In this procedure, approximately 40 mg of $\text{HAuCl}_4 \cdot 3\text{H}_2\text{O}$ was taken in 7.5 mL of THF and ~65 mg of tetraoctylammonium bromide (TOAB) was added and stirred for about 15 min to get a deep red solution. Then 5 mole equivalents (with respect to gold) of PET were added and the solution was stirred for about an hour to get a colorless solution indicating the formation of Au-SR thiolate mixtures. These thiolates were reduced by the addition of ~39 mg of NaBH_4 in 2.5 mL of ice cold water and the reaction was stirred for another 6 h to get a reddish brown colored solution. The entire synthesis was carried out at room temperature and stirring speed was kept at ~1500 rpm. THF was then evaporated by vacuum drying and the cluster was precipitated to remove excess thiol and other impurities which were discarded with the supernatant solution. This step was repeated 2-3 times followed by extraction of the $\text{Au}_{25}(\text{PET})_{18}$ cluster in acetone leaving behind bigger particles. Finally the pure cluster was extracted in DCM.

Synthesis of $\text{Ir}_9(\text{PET})_6$: This cluster was synthesized following a recently reported solid state protocol.² Briefly, $\text{IrCl}_3 \cdot x\text{H}_2\text{O}$ and PET in 1:4 molar ratios were mixed together by grinding in a mortar and pestle to form Ir thiolates which are yellow in color. Then these thiolates were reduced by the addition of ~30 mg of NaBH_4 and grinding the mixture till the color changes from yellow to blackish indicating the formation of the desired cluster. The cluster was then extracted in toluene which was evaporated using vacuum drying and the cluster was precipitated by the addition of excess methanol to remove thiol and other impurities. This procedure was repeated for 2-3 times to get pure cluster.

Separation by Thin Layer Chromatography (TLC): Around 1 μL of cluster solution was spotted on TLC plate and dried in air. The mobile phase used for the elution was 60:40 (v/v) DCM:hexane. The plate was eluted and separated bands were cut from the TLC plate. Then these bands were extracted in DCM and centrifuged to remove residues of the TLC plate.

Supporting information 2

Instrumentation:

UV/Vis spectroscopy: UV/Vis spectra were collected using Perkin Elmer Lambda 25 instrument with a range of 200 – 1100 nm with a band pass filter of 1 nm.

MALDI MS: MALDI MS of Ir₉(PET)₆ cluster was measured using a Voyager-DE PRO Biospectrometry Workstation from Applied Biosystems. DHB matrix was used in the ratio of 1:100 of sample:matrix. Appropriate volumes of sample were spotted on the plate and allowed to dry under ambient condition. A 337 nm nitrogen laser was used for desorption and ionization. Mass spectra were collected in linear positive ion mode and were averaged for 250 shots. Accelerating voltage was kept at 20 kV. The measurements were done at threshold laser intensity.

ESI MS: The ESI MS were measured in Waters' Synapt G2Si HDMS instrument. The Synapt instrument consists of an electrospray source, quadrupole ion guide/trap, ion mobility cell, and TOF detector. Different gases are used in different parts of the instrument. Nitrogen gas is used as the nebulizer gas. All the experiments were done in positive ion mode using CsOAC as an ionization enhancer. Cluster was mixed with 50 mM CsOAC at 1:1(v/v) ratio before infusing to the ESI MS system. The optimized conditions for a well resolved MS were as follows:

Sample concentration: 10 µg/mL

Solvent: DCM

Flow rate: 30 µL/min

Capillary voltage: 3.5 kV

Cone voltage: 120-150 V

Source offset: 80-120 V

Desolvation gas flow: 400 L/h

Trap gas flow: 5 mL/min

Computational Details: The structure of Au₂₅(SR)₁₈ used was from the report of Heaven *et al.*³ (Figure S4). Different possible structures have been obtained with the systematic substitution of Ir atoms with Au. The PET ligands were replaced with methyl groups to

reduce the computational cost. Such simplification has been often used in previous calculations to reduce the computational burden and is acceptable.⁴ The geometries with Ir substitution were optimized using density functional theory (DFT) method. Perdew, Burke, and Ernzerhof (PBE) functional was used to locate the stationary points on the potential energy surface. For Au and Ir atoms, LANL2DZ basis set was used and 6-31G* was used for the rest of the atoms (S, C and H). All the calculations were performed using Gaussian 09 software.⁵

To investigate the absorption spectrum of $\text{Au}_{22}\text{Ir}_3(\text{SCH}_3)_{18}$, time-dependent density functional theory (TDDFT) calculations have been performed on the lowest energy geometry of $\text{Au}_{22}\text{Ir}_3(\text{SMe})_{18}$ using PBE1PBE level of theory for 400 excitations. Gold and Iridium were treated with LANL2DZ basis set and carbon, sulphur and hydrogen with 6-31G*. The calculated spectrum was broadened using Lorentzian method.

Supporting information 3

Characterization of $\text{Au}_{25}(\text{PET})_{18}^-$:

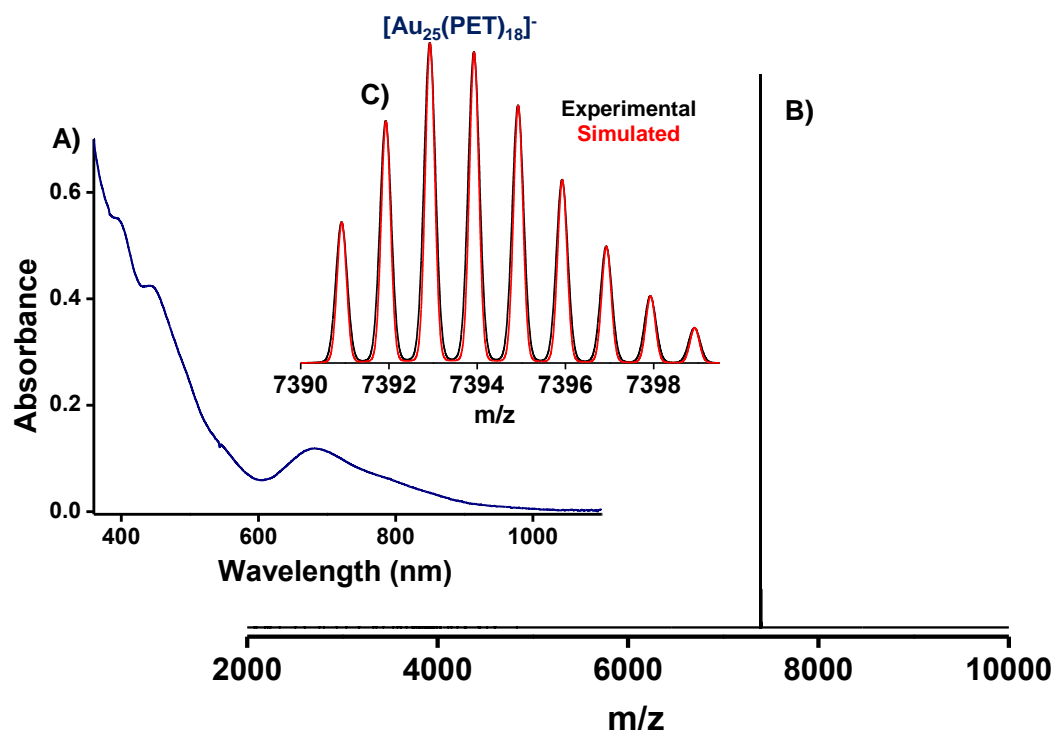


Figure S1: A) Optical absorption spectrum of $[\text{Au}_{25}(\text{PET})_{18}]^-$ in DCM. B) Negative ion mode ESI MS of $[\text{Au}_{25}(\text{PET})_{18}]^-$. C) Experimental (black trace) and simulated (red trace) mass spectrum of the $[\text{Au}_{25}(\text{PET})_{18}]^-$ species.

Supporting information 4

Characterization of $\text{Ir}_9(\text{PET})_6$:

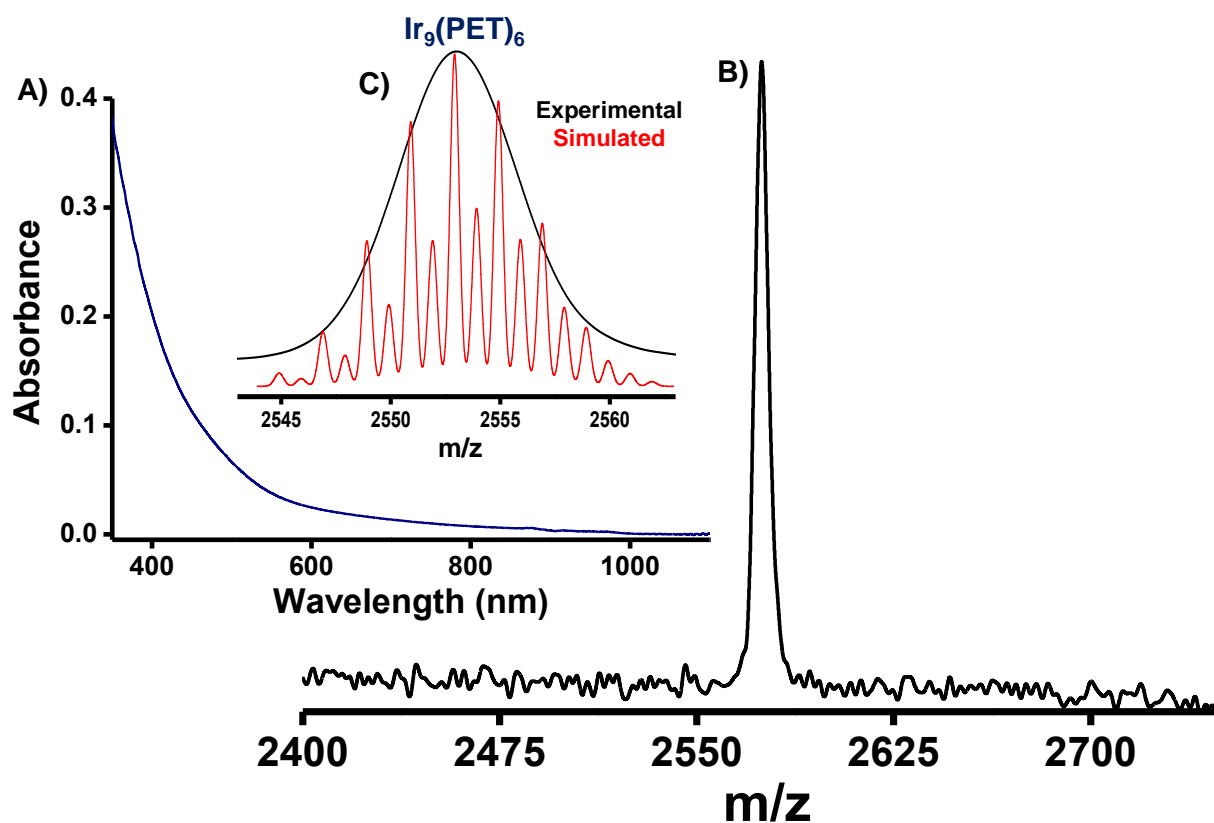


Figure S2: A) Optical absorption spectrum of $\text{Ir}_9(\text{PET})_6$. B) Positive ion mode MALDI MS of $\text{Ir}_9(\text{PET})_6$. C) Experimental (black trace) and simulated (red trace) mass spectrum for $[\text{Ir}_9(\text{PET})_6]^+$ species.

Supporting Information 5

Effect of reactant concentration on the reaction:

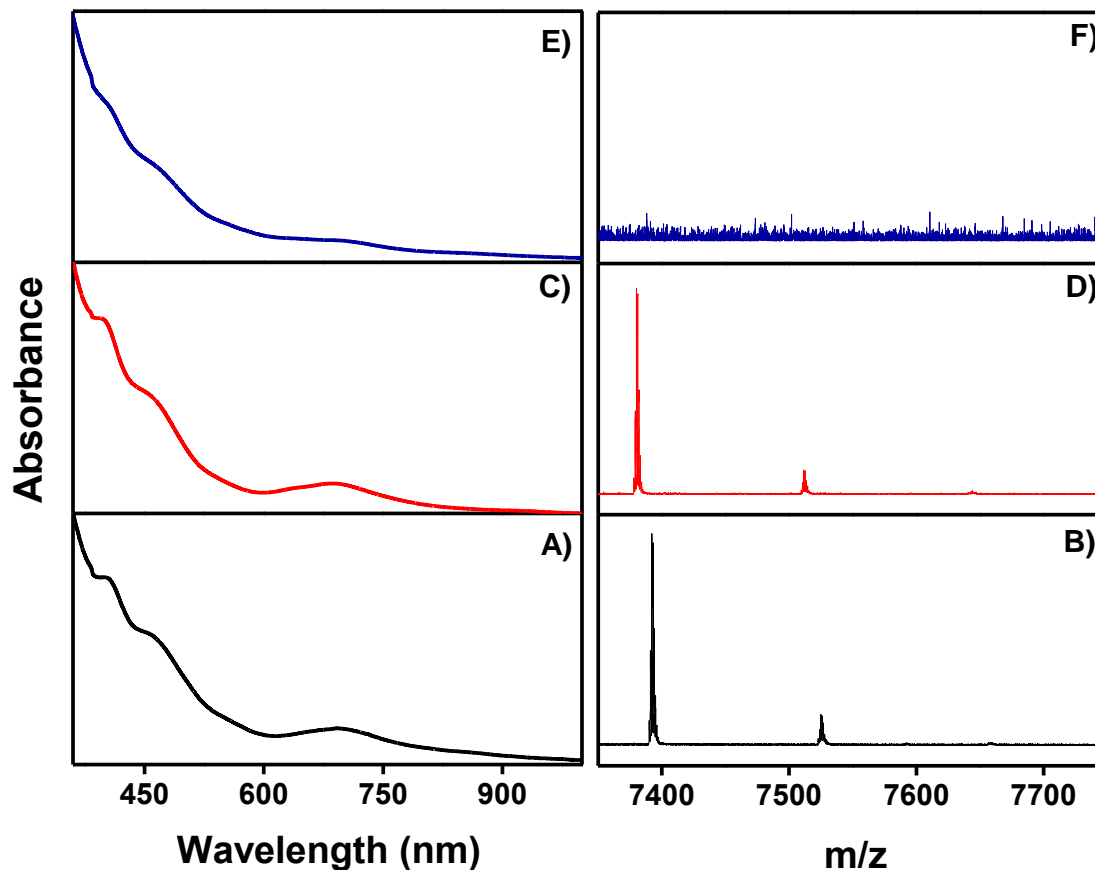


Figure S3: (A) Optical absorption spectrum and (B) positive ion mode ESI MS of reaction mixture containing 1.0:0.5 (v/v) of $\text{Au}_{25}(\text{PET})_{18}:\text{Ir}_9(\text{PET})_6$, after 24 h of stirring. (C) Optical absorption spectrum and (D) positive ion mode ESI MS of reaction mixture containing 1.0:1.0 (v/v) of $\text{Au}_{25}(\text{PET})_{18}:\text{Ir}_9(\text{PET})_6$, after 24 h of stirring. (E) Optical absorption spectrum and (F) positive ion mode ESI MS of reaction mixture containing 1.0:1.5 (v/v) of $\text{Au}_{25}(\text{PET})_{18}:\text{Ir}_9(\text{PET})_6$, after 24 h of stirring.

Supporting Information 6

Structure of $\text{Au}_{25}(\text{SMe})_{18}$:

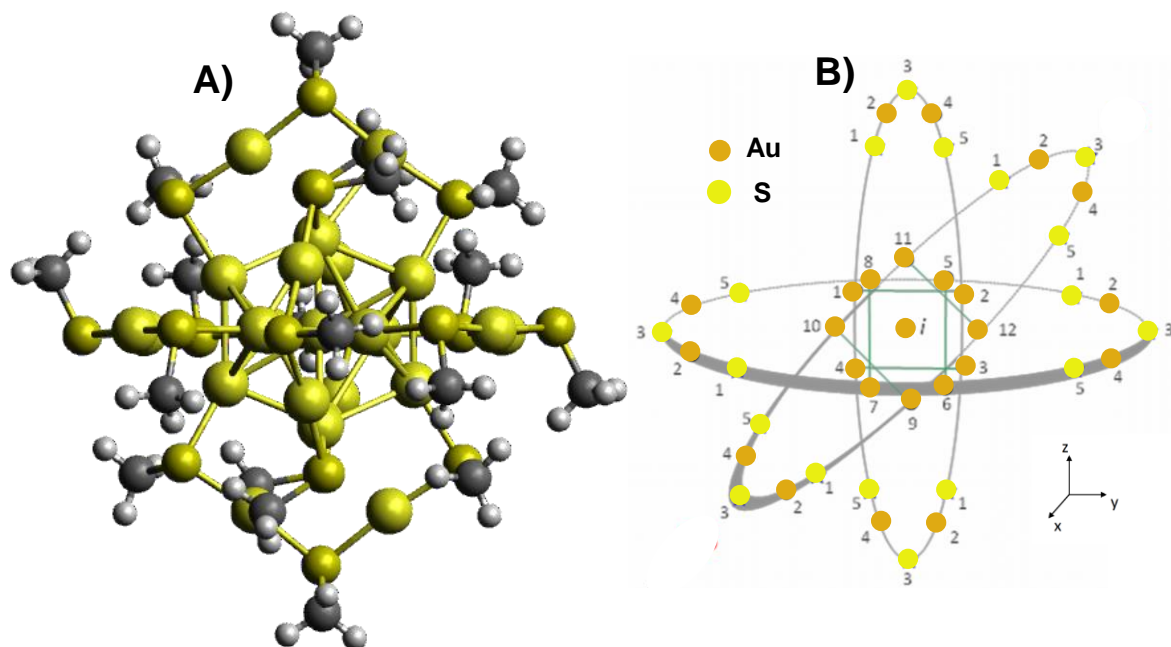


Figure S4: Structure of $\text{Au}_{25}(\text{SMe})_{18}$ with its aspicule representation. Color Code: Dark yellow-Au, bright yellow-S, gray-C and white-H.

Supporting Information 7

DFT optimized structures of $\text{Au}_{24}\text{Ir}(\text{SMe})_{18}$ and $\text{Au}_{23}\text{Ir}_2(\text{SMe})_{18}$:

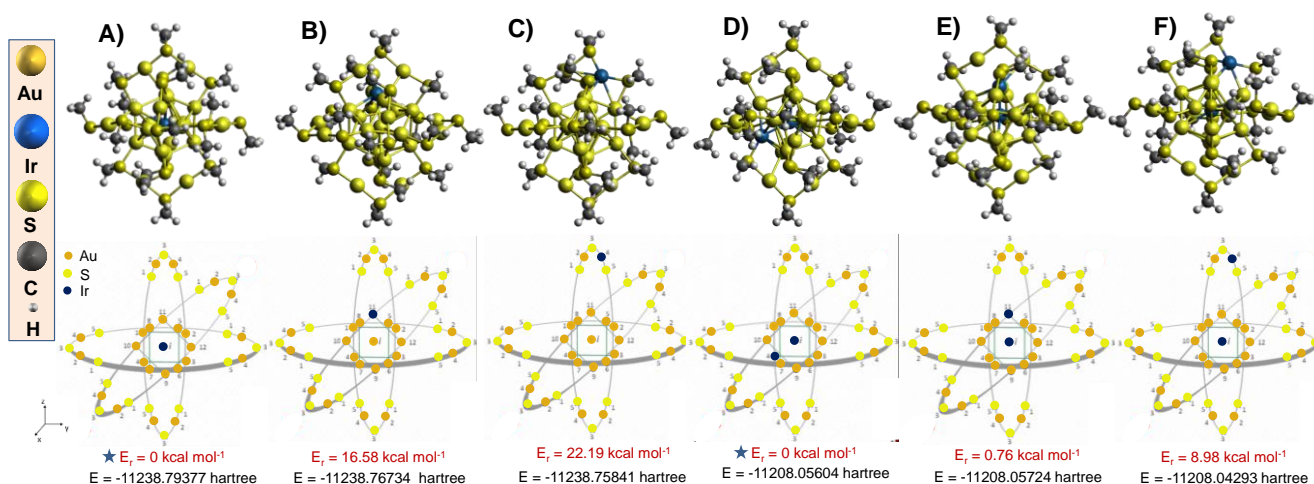


Figure S5. DFT optimized structures of A), B), C) isomers of $\text{Au}_{24}\text{Ir}(\text{SMe})_{18}$ and E), F), G) selected isomers of $\text{Au}_{23}\text{Ir}_2(\text{SMe})_{18}$. The aspicule representation of each structure is given below the structures. The positions of Ir are labelled prominently. In case of isomers of one Ir substituted structures, the relative energies are calculated with respect to structure A and in case of two Ir substituted structures; relative energies are calculated with respect to structure D. Color code: Golden yellow – Au; bright yellow – S; blue – Ir; gray – C and white –H.

Supporting Information 8

DFT optimized structures of lower energy isomers of $\text{Au}_{22}\text{Ir}_3(\text{SMe})_{18}$:

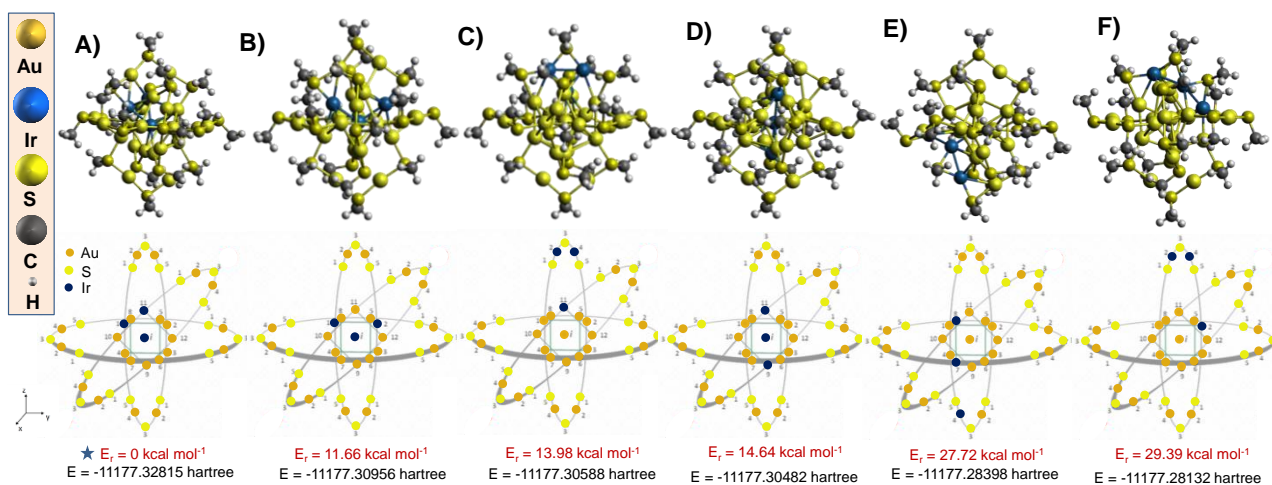


Figure S6. DFT optimized structures of most stable geometries (with formation Ir_3 units) and their isomers of $\text{Au}_{22}\text{Ir}_3(\text{SMe})_{18}$. Aspicule representations of the structures are given below the respective structure. The relative energies are calculated with respect to isomer A. The most stable structure is highlighted with an asterisk. Color code: Dark yellow – Au; bright yellow – S; blue – Ir; grey – C and white – H.

Supporting Information 9

DFT optimized structures of higher energy isomers of $\text{Au}_{22}\text{Ir}_3(\text{SMe})_{18}$:

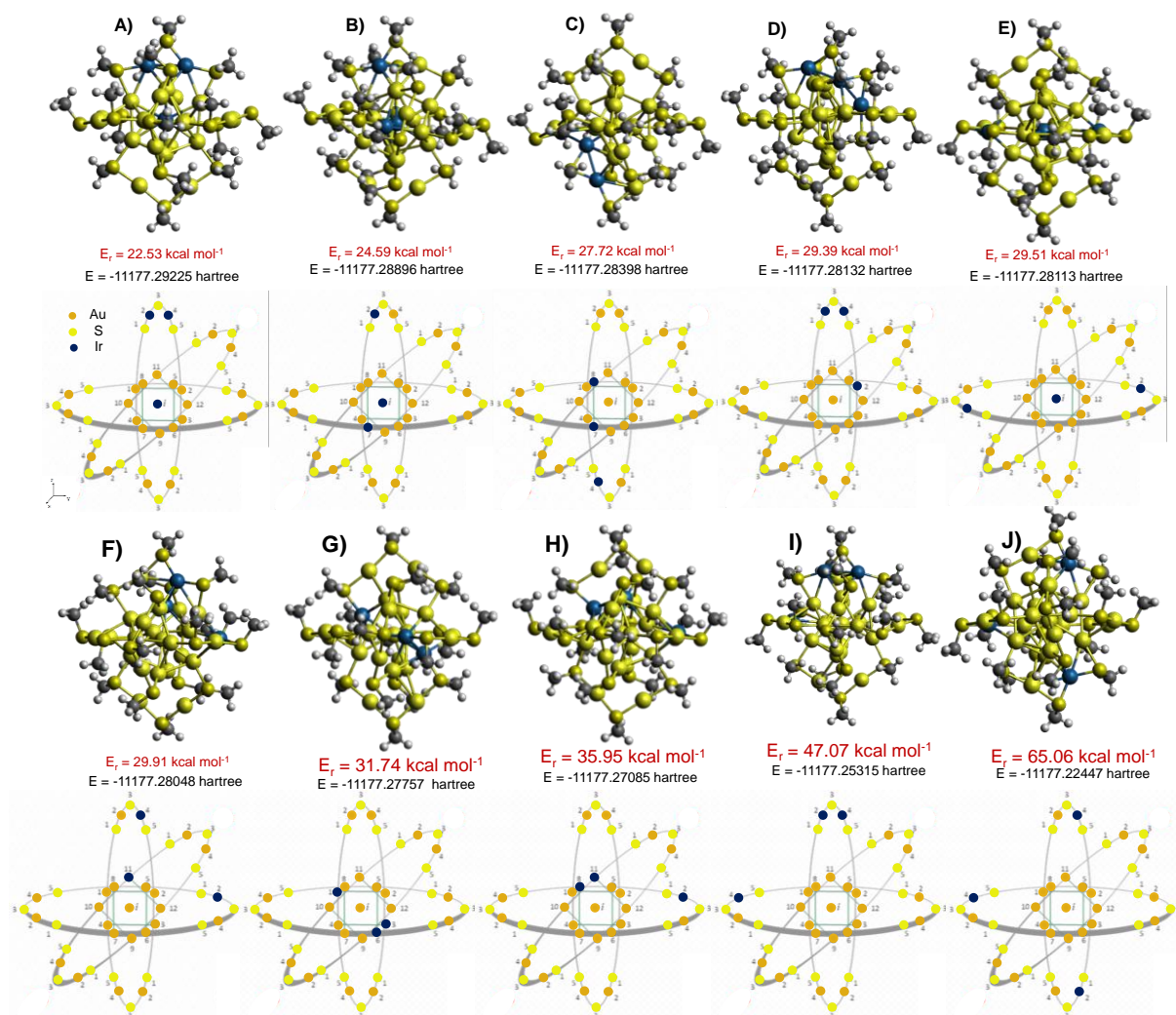


Figure S7. DFT optimized structures of few random higher energy isomers of $\text{Au}_{22}\text{Ir}_3(\text{SMe})_{18}$. The aspicule representation of each structure is given below respective structure. The relative energies are calculated with respect to structure A in Figure S6. Color code: Dark yellow – Au, bright yellow – S, blue – Ir, gray – C and white – H.

Supporting Information 10

Results of DFT calculations:

Table S1: Isomers of $\text{Au}_{24}\text{Ir}(\text{SMe})_{18}$ and their energies:

No.	Position of Ir atom	Absolute energy (hartree)	Relative energy (kcal mol^{-1})*
1	Center of the icosahedron	-11238.79377	0.00
2	Shell of the icosahedron	-11238.76734	16.58
3	Staple	-11238.75841	22.19

Table S2: Isomers of $\text{Au}_{23}\text{Ir}_2(\text{SMe})_{18}$ and their energies:

No.	Position of Ir atoms	Absolute energy (hartree)	Relative energy (kcal mol^{-1})*
1	One in center and one in shell of the icosahedron	-11208.05604	0.00
2	One in center and one in shell of the icosahedron	-11208.05724	0.76
3	One in center of the icosahedron and one in staple	-11208.04293	8.98

Table S3: Isomers of $\text{Au}_{22}\text{Ir}_3(\text{SMe})_{18}$ with Ir_3 units and their energies. Their structures are shown in Figure 4 and S6.

No.	Position of Ir atoms	Absolute energy (hartree)	Relative energy (kcal mol^{-1})*
1	One in center and two in shell of the icosahedron forming Ir_3 triangular unit	-11177.32815	0.00
2	One in center and two in shell of the icosahedron forming angular Ir_3 unit	-11177.30956	11.66

3	One in shell of icosahedron and two in same staple forming triangular Ir ₃ unit	-11177.30588	13.98
4	One in center and two in shell of icosahedron forming a linear Ir ₃ unit	-11177.30482	14.64
5	Two in shell of icosahedron and one in staple forming an Ir ₃ unit	-11177.28398	27.72
6	Two in same staple and one in the shell of the icosahedron forming an Ir ₃ unit	-11177.28132	29.39

Table S4: Isomers of Au₂₂Ir₃(SMe)₁₈ without Ir₃ unit and their energies. Their structures are shown in Figure S7.

7	One in center of the icosahedron and two in same staple	-11177.29225	22.53
8	One in center, one in shell of the icosahedron and one in staple	-11177.28896	24.59
9	One in center of the icosahedron and two in different staples, no bonding between Ir atoms	-11177.28113	29.51
10	One in the shell of the icosahedron and two in different staples with one Ir – Ir bond	-11177.28048	29.91
11	Three Ir in the shell of the icosahedron with one Ir – Ir bond	-11177.27757	31.74
12	Two in shell of icosahedron and one in staple with one Ir – Ir bond	-11177.27085	35.95
13	Two in same staple and one in different with one Ir – Ir bond	-11177.25315	47.07
14	Three in different staples	-11177.22447	65.06

*Note: Relative energies are calculated with respect to 1st isomer in each case.

Supporting Information 11

Result of TDDFT calculations:

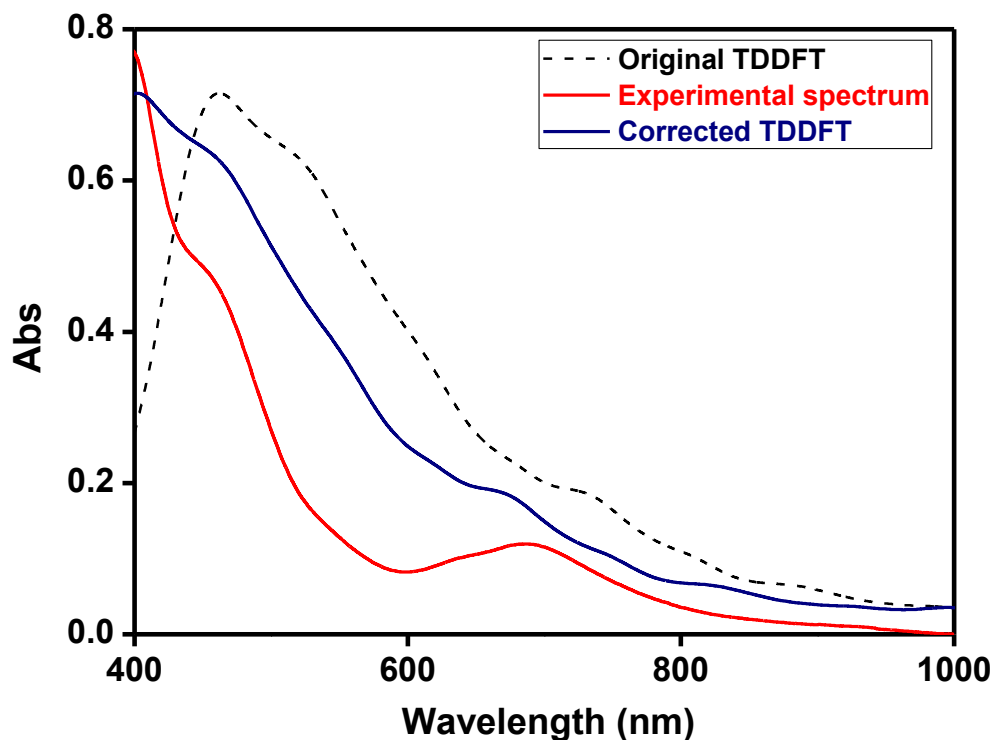


Figure S8. TDDFT calculated UV/Vis absorption spectrum for most stable isomer of $\text{Au}_{22}\text{Ir}_3(\text{PET})_{18}$ cluster (black dotted trace) compared with the experimental UV/Vis spectrum (red trace). The TDDFT calculated spectrum shows a shift of ~ 60 nm which is corrected and plotted as blue trace. This shift is due to the simplifications such as replacement of PET ligands by SMe ligands and consideration of effective core potentials for Au and Ir atoms in TDDFT calculation.

References:

1. Wu, Z.; Suhan, J.; Jin, R., One-pot synthesis of atomically monodisperse, thiol-functionalized Au₂₅ nanoclusters. *J. Mater. Chem.* 2009, *19* (5), 622-626.
2. Bhat, S.; Chakraborty, I.; Maark, T. A.; Mitra, A.; De, G.; Pradeep, T., Atomically precise and monolayer protected iridium clusters in solution. *RSC Adv.* 2016, *6* (32), 26679-26688.
3. Heaven, M. W.; Dass, A.; White, P. S.; Holt, K. M.; Murray, R. W., Crystal Structure of the Gold Nanoparticle [N(C₈H₁₇)₄][Au₂₅(SCH₂CH₂Ph)₁₈]. *J. Am. Chem. Soc.* 2008, *130* (12), 3754-3755.
4. Iwasa, T.; Nobusada, K., Theoretical Investigation of Optimized Structures of Thiolated Gold Cluster [Au₂₅(SCH₃)₁₈]⁺. *J. Phys. Chem. C* 2007, *111* (1), 45-49.
5. Frisch, M. J. T., G. W. Schlegel, H. B. Scuseria, G. E. Robb, M. A. Cheeseman, J. R., et al., Gaussian 09 A 02, Gaussian, Inc., Wallingford CT, 2009.